Dynamics of molecule-surface interactions from first principles

Axel Groß
Physik-Department T30, TU München, 85747 Garching, Germany
(Dated: March 5, 2003)

Total-energy calculations based on *ab initio* electronic structure theory can nowadays yield the multidimensional potential energy surfaces of simple molecules interacting with surfaces in great detail. For the dissociation of hydrogen molecules on metal surfaces, these calculations have motivated high-dimensional quantum dynamical simulations of adsorption and desorption dynamics based on *ab initio* potential energy surfaces in which all hydrogen degrees of freedom were treated explicitly while the metal surface was usually kept fixed. These dynamical studies demonstrated in particular the importance of the multidimensionality of the reaction dynamics not only for a quantitative, but also for a qualitative understanding of the underlying microscopic processes. *Ab initio* molecular dynamics simulations have also addressed adsorption systems in which the substrate degrees of freedom play a crucial role, such as adsorption on semiconductor surfaces or molecular trapping. While all these simulations rely on the Born-Oppenheimer approximation, first attempts have already been made to address the interaction dynamics with electronic transitions at surfaces from first principles.

Keywords: Molecular dynamics; Computer simulations; Density functional theory; Chemisorption; Sticking; Thermal desorption; Desorption induced by photon stimulation; Hydrogen molecule; Oxygen; Low index single crystal surfaces

I. INTRODUCTION

The last years have witnessed tremendous progress in the theoretical description of surfaces and processes on surfaces. A variety of surface properties can now be described from first principles, i.e. without invoking any empirical parameters [1]. In particular, whole potential energy surfaces (PES) can nowadays be mapped out by total energy calculations based on *ab initio* electronic structure theory. These development has also motivated new efforts in the dynamical treatment of adsorption/desorption processes in the last decade such as the development of efficient schemes for high-dimensional quantum dynamical simulations [2, 3].

Before *ab initio* potential energy surfaces became available, usually the interaction potential between the molecule and the surface had been based on educated guesses or simplified model potentials. Since the complexity of a PES increases significantly with its dimensionality, guessing a, e.g., six-dimensional realistic PES for a diatomic molecule in front of a surface is almost impossible. Low-dimensional simulations can still yield important qualitative insights in certain aspects of the adsorption/desorption dynamics [4], but they do not allow the quantitative determination of reaction probabilities. Moreover, certain qualitative mechanisms are only operative in a realistic multidimensional treatment.

In fact, the potential energy surfaces derived from *ab initio* electronic structure calculations demonstrated that the corrugation and anisotropy of the interaction potentials of molecules with surfaces, even with low-index metal surfaces, are much larger than previously assumed. Using these potential energy surfaces in realistic dynamical simulations confirmed the importance of taking the appropriate multidimensionality of the interaction dynamics into account [2, 3].

In this contribution I will review dynamical studies of molecular adsorption and desorption from metal and semiconductor surfaces based on potential energy surfaces that were derived from first-principles electronic structure calculations. In many cases these dynamical simulations are in quantitative agreement with available experiments. Still it is the advantage of simulations compared to the experiment that the time evolution of wave packets or trajectories can be followed in any moment. This makes a determination and analysis of the crucial qualitative mechanisms governing the interaction dynamics possible. Thus the high-dimensional simulations based on *ab initio* electronic structure calculations do not only yield a quantitative, but sometimes also a novel qualitative understanding of the adsorption and desorption dynamics. One prominent example is the concept of dynamical steering [5] whose importance in particular at low kinetic energies was underestimated for a long time.

Before a detailed presentation of the *ab initio* dynamics simulations, first the fundamental difference between atomic and molecular adsorption on the one hand and dissociative adsorption on the other hand has to be addressed. Then I will briefly discuss the question whether quantum or classical methods are appropriate for the simulation of the adsorption dynamics. This section will be followed by a short introduction into the determination of potential energy surfaces from first principles and their continuous representation by some analytical or numerical interpolation schemes. Then the dissociative adsorption and associative desorption of hydrogen at metal and semiconductor surfaces and the molecular trapping of oxygen on platinum will be discussed in some detail. Finally I address some first attempts to incorporate electronic excitations in dynamical simulations from first principles. This review ends with an outlook at the promising prospects for realistic high-dimensional

simulations. More and more complex systems will be addressed by *ab initio* molecular dynamics simulations deepening our microscopic understanding of many fundamentally and technolgically important processes at surfaces.

II. FUNDAMENTALS OF MOLECULAR AND DISSOCIATIVE ADSORPTION

In the adsorption of atoms and molecules at surfaces one usually distinguishes between chemisorption and physisorption depending on whether or not true chemical bonds between substrate and adsorbate are formed. Both cases still correspond to a bond-making process even if the bond is relatively weak, as it is typical for physisorption systems where the attraction is caused by van der Waals forces. The bonding state is in general characterized by a lower energy than the separated system. Thus the adsorbate-substrate bond can only be formed if the adsorption system can get rid of the energy gained upon the adsorption, i.e., if the excess energy can be dissipated. This is similar to gas-phase reactions where a bond between two reactants can only be formed in a three-body collision where a third reaction partner has to carry away the energy gained by the reaction unless there are other dissipation channels such as radiation.

However, reactions at surfaces differ from gas-phase reactions insofar as the whole substrate can serve as an efficient energy sink. There are two main channels for energy dissipation, namely phonon and electron-hole pair excitations. In fact, the theorectical description of both dissipation mechanisms upon adsorption from first principles still represents a challenge. On the one hand, the modelling of phonon excitations in the molecule-surface collision usually requires the consideration of large systems which is computationally rather demanding. On the other hand, electronic structure theory for extended systems has not matured enough yet in order to provide a reliable, computationally feasible scheme for the determination of electronically excited states which is necessary for the description of electron-hole pairs. However, there are promising approaches that will be discussed in this review.

The sticking or adsorption probability is defined as the fraction of atoms or molecules impinging on a surface that are not scattered back, i.e. that remain on the surface. For the explicit evaluation of sticking probabilities, we first define $P_E(\epsilon)$ as the probability that an incoming particle with kinetic energy E will transfer the energy ϵ to the surface. In order to remain at the surface, the particle has to transfer more than its initial energy to the substrate excitations, i.e., the sticking probability can be expressed as

$$S(E) = \int_E^\infty P_E(\epsilon)\, d\epsilon. \tag{1}$$

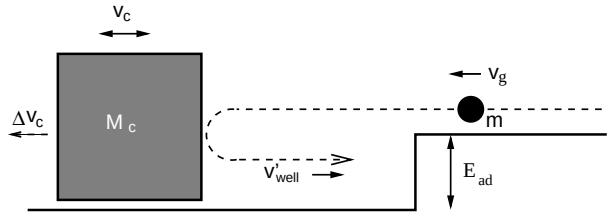

FIG. 1: Schematic illustration of the hard-cube model. An atom or molecule with mass m is impinging in an attractive potential with well depth $E_{\rm ad}$ on a surface modeled by a cube of effective mass M_c. The surface cube is moving with a velocity v_c given by a Maxwellian distribution.

There is a very simple model for estimating the trapping probability in atomic adsorption due to a phonon-excitation mechanism. In the *hard-cube model* (HCM) [6, 7], the impact of the atom on the surface is treated as a binary elastic collision between a gas phase atom (mass m) and a substrate atom (mass M_c) which is moving freely with a velocity distribution $P_c(v_c)$. This model is schematically illustrated in Fig. 1. If the depth of the adsorption well is denoted by $E_{\rm ad}$, the adsorbate will impinge on the hard cube with a velocity

$$v_{\rm well} = -\sqrt{v_{\rm g}^2 + \frac{2E_{\rm ad}}{m}}. \tag{2}$$

Assuming a weighted Maxwellian velocity distribution for v_c, the trapping probability in the hard-cube model can be analytically expressed as [7]

$$S_{\rm trap}(v_{\rm g}) = \frac{1}{2} + \frac{1}{2}\,{\rm erf}(\alpha v_{\rm lim}) + \frac{\exp\left\{-\alpha^2 v_{\rm lim}^2\right\}}{2\sqrt{\pi}\alpha v_{\rm well}}\ , \tag{3}$$

where $\alpha = \sqrt{M_c/2k_{\rm B}T_{\rm s}}$, $v_{\rm lim}$ is given by

$$v_{\rm lim} \ = \ \frac{\mu+1}{2}\sqrt{\frac{2E_{\rm ad}}{m}} - \frac{\mu-1}{2}v_{\rm well}\ , \tag{4}$$

and μ is the mass ratio $\mu = m/M$.

When an atom hits a surface, the initial kinetic energy of the atom can not only be transfered to the substrate. If the surface is corrugated, i.e., if the atom-surface interaction varies as a function of lateral coordinates of the atom, then the impinging atom can also change its lateral component of the initial velocity upon the collision. In the case of molecules, there are also the internal degrees of molecular vibration and rotation that can be excited (or de-excited) during the collision with the surface.

Eventually any adsorbed atom or molecule will equilibrate with the surface which means that the mean energy in the lateral and internal degrees of freedom of the adsorbate will correspond to the surface temperature. Hence any excess energy in these degrees of freedom will be dissipated to the substrate. Still the temporary excitation of lateral motion and internal degrees of freedom in the adsorption process can be very important for the magnitude of the sticking probability. The energy stored in

these additional degrees of freedom is not available for a direct escape from the adsorption well. If enough of the initial perpendicular kinetic energy is transfered in the first collision into these other degrees of freedom, the molecule becomes dynamically trapped for a while [8, 9]. While being trapped, the molecule can hit the surface several times and transfer successively more and more energy to the substrate until it equilibrates. This mechanism, which will be treated in detail in the section about the adsorption of O_2 on Pt(111), is not described at all by the hard-cube model which assumes a projectile without any internal degrees of freedom colliding with a flat surface.

In the case of dissociative adsorption on surfaces there is an additional channel into which energy can be transfered, namely the conversion of the kinetic and internal energy of the molecule into translational energy of the fragments on the surface with respect to each other. In fact, in the dissociation of light molecules such as H_2 on metal surfaces the dissociative adsorption probability is almost entirely determined by the initial H-H bond-breaking process. The surface does not participate dynamically in this dissociation process because of the large mass mismatch between the substrate atoms and the impinging molecule and due to the fact that metal surfaces usually do not exhibit a strong surface rearrangement upon adsorption. Thus the dissociative adsorption process can be described within the low-dimensional framework of only the molecular degrees of freedom. The determination of the sticking probability can be expressed as a transmission/reflection problem where the dissociative adsorption probability is given by the probability to enter the dissociation channel. Of course, the molecular fragments will eventually accommodate at the surface, however, this process is not relevant for the dissociative adsorption and is therefore usually not considered in the dynamical simulations.

This is different at semiconductor surfaces where the covalent bonds between the substrate atoms are often strongly perturbed by the presence of adsorbates. This can result in a significant surface restructuring. Hence the dynamics of the substrate atoms has to be explicitly taken into account which of course increases the complexity of the modelling of the adsorption/desorption dynamics, as will be shown below for the H_2/Si system.

III. QUANTUM DYNAMICS VERSUS CLASSICAL DYNAMICS

The interaction between a molecule and a surface is governed by the forces acting between the electrons and nuclei of the whole system. Due to their light mass, the electrons have to be treated quantum mechanically. However, because of their large mass the nuclei hardly move on the time scale typical for the electron dynamics. Therefore it is reasonable to assume that the electrons follow the slow motion of the nuclei adiabatically. This so-called Born-Oppenheimer or adiabatic approximation allows the separation of the electronic and nuclei degrees of freedoms in the solution of the Schrödinger equation. First one solves the electronic many-body Schrödinger equation using a Hamiltonian where the positions of the nuclei just enter as fixed external parameters.

Usually one assumes that the electrons stay in their ground state. The ground-state energy of the electronic Hamiltonian as a function of the nuclear coordinates then represents the potential energy surface describing the interaction of a molecule with a substrate. Of course all electronic transitions are neglected in this ansatz. Often this is a reasonable assumption although its validity is hard to prove. Still, there is an important class of dynamical processes on surfaces which involve electronic transitions. I will also briefly discuss such processes later in this review.

Once the potential energy surface is available, the dynamics of the nuclei can be simulated. The appropriate method would again be the solution of the Schrödinger equation, now for the nuclear coordinates. Unfortunately, this can only be done for a limited number of freedoms. As mentioned in the previous section, in the interaction of hydrogen molecules with close-packed metal surfaces the substrate atoms do usually not participate in the dissociation process. Still there are six molecular degrees of freedom left. While a decade ago it was still not possible to perform full quantum dynamical simulations in all hydrogen degrees of freedom, this can now be routinely done by several groups [5, 10–13]. Even one additional surface oscillator coordinate has been included in full quantun dynamical simulations [14].

Nevertheless, the computational effort required for quantum dynamical simulations scales very unfavorably with the number of degrees considered. In addition, for heavier atoms quantum calculations also become more costly. However, for atoms heavier than hydrogen or deuterium the quantum effects in the dynamics are often negligible [2]. Hence it is usually justified to perform classical molecular dynamics simulations for these heavier atoms. In fact, even in the hydrogen adsorption/desorption dynamics many integrated quantities such as the sticking probability which corresponds to an average over all possible initial molecular configuration can be semi-quantitatively or even quantitatively determined by classical dynamics [15–17]. If the microscopic dynamics of many substrate atoms should be explicitly included in the dynamical simulation, then there is anyhow no alternative to classical dynamics simulations at the moment.

IV. DETERMINATION OF POTENTIAL ENERGY SURFACES

The potential energy surface is the central quantity in the discussion and analysis of the dynamics of a reaction. Its determination requires the solution of the many-body electronic Schrödinger equation. While in the early days

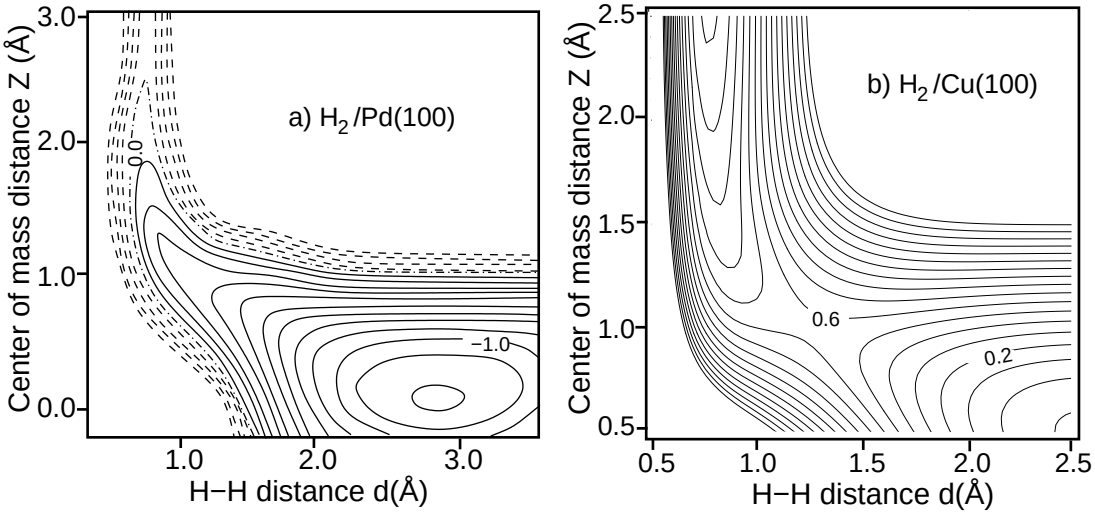

FIG. 2: Contour plots of the potential energy surface along two-dimensional cuts through the six-dimensional coordinate space of H_2 in front of (100) metal surfaces determined by DFT-GGA calculations in the h–b–h geometry. The contour spacing is 0.1 eV per H_2 molecule. (**a**) H_2/Pd(100) (after [18]), (**b**) H_2/Cu(100) [19].

of theoretical surface science quantum chemical methods had a significant impact, nowadays electronic structure calculations using density functional theory (DFT) [20, 21] are predominantly used. DFT is based on the fact that the exact ground state density and energy can be determined by the minimisation of the energy functional $E[n]$:

$$E_{\rm tot} = \min_{n(\vec{r})} E[n] = \min_{n(\vec{r})}(T[n] + V_{\rm ext}[n] + V_{\rm H}[n] + E_{\rm xc}[n]) \ . \tag{5}$$

$V_{\rm ext}[n]$ and $V_H[n]$ are the functionals of the external potential and of the classical electrostatic interaction energy, respectively, while $T[n]$ is the kinetic energy functional for non-interacting electrons. All quantum mechanical many-body effects are contained in the so-called exchange-correlation functional $E^{\rm xc}[n]$.

In most present implementation of DFT, the many-body Schrödinger equation is replaced by a set of coupled effective one-particle equations, the so-called Kohn-Sham equations [21]

$$\left\{ -\frac{\hbar^2}{2m}\nabla^2 + v_{ext}(\vec{r}) + v_{\rm H}(\vec{r}) \ + \ v_{\rm xc}(\vec{r}) \right\} \psi_i(\vec{r}) = \varepsilon_i \, \psi_i(\vec{r}) \ , \tag{6}$$

where $v_{\rm ext}$ is the external potential and the *Hartree potential* $v_{\rm H}$ is given by

$$v_{\rm H}(\vec{r}) = \int d^3\vec{r}' n(\vec{r}') \frac{e^2}{|\vec{r} - \vec{r}'|} \ . \tag{7}$$

The exchange-correlation potential $v_{\rm xc}(\vec{r})$ is the functional derivative of the exchange-correlation functional $E_{\rm xc}[n]$

$$v_{\rm xc}(\vec{r}) = \frac{\delta E_{\rm xc}[n]}{\delta n} \ . \tag{8}$$

The electron density $n(\mathbf{r})$ which minimizes the total energy is then given by the sum over single-particle Kohn-Sham states

$$n(\vec{r}) = \sum_{i=1}^{N} \ |\psi_i(\vec{r})|^2 \ . \tag{9}$$

As eqs. (6)–(9) show, the solutions $\psi_i(\vec{r})$ of the Kohn-Sham equations do in fact enter the effective one-particle Hamiltonian. In such a situation, the set of one-particle equations can only be solved in an iterative fashion: One starts with some initial guess for the wave functions which determine the effective one-particle Hamiltonian. The Kohn-Sham equations are then solved and a new set of solutions is determined. This cycle is repeated so often until the iterations no longer modify the solutions, i.e. until self-consistency is reached. Of particular importance for the reliability of the DFT calculations is the specific form of the exchange-correlation functional. In principle DFT is exact, however, the exact form of the correct exchange-correlation functional is unfortunately not known so that approximative expressions are needed. While the so-called local density approximation has been surprisingly successful for bulk properties, it is not sufficiently accurate to describe reactions at surfaces [22]. In the generalized gradient approximation (GGA) the gradient of the density is also taken into account in the exchange-correlation functional [23]. GGA calculations give satisfactory results for many adsorbate systems but there are still important exceptions [24].

Using efficient DFT codes, whole potential energy surfaces of the interaction of molecules with surface can be mapped out in great detail. Figure 2 presents two-dimensional cuts through the six-dimensional configuration space, so-called elbow plots of two benchmark systems, namely H_2/Pd(100) and H_2/Cu(100). In these

plots, the PES is shown as a function of the hydrogen distance from the surface Z and the intramolecular H-H spacing d; the molecular orientation and lateral position are kept fixed. Both plots in Fig. 2 correspond to the so-called h–b–h geometry with the molecular center of mass above the bridge site and the atoms oriented towards the adjacent fourfold hollow sites. The interaction of H_2 with palladium represents the standard example for non-activated dissociative adsorption [25]. As Fig. 2a demonstrates, H_2 can spontaneously dissociate on Pd(100) since there is no barrier along the reaction path from the molecule in the gas phase (upper left corner of the plot) to the dissociatively adsorbed molecule on the surface (lower right corner). H_2/Cu used to be *the* model system for the study of the dynamics of dissociative adsorption and associative desorption in the last decade [4, 10, 13, 26–34]. In this system, the dissociative adsorption is hindered by an energetic barrier whose height is 0.5–0.6 eV (Fig. 2b).

It is important to note that DFT total-energy calculations do not provide a continuous potential energy surface, as one might naively assume from the inspection of Fig. 2. In fact, the elbow plots shown are based on a series of 50–100 DFT calculations with varying center of mass and H-H distance. The continuous representation is just a result of a contour plot routine that interpolates between the actually calculated energies.

For any dynamical simulation, a continuous representation of the PES is mandatory since the potential and the gradients are needed for arbitrary configurations. One can in fact perform *ab initio* molecular dynamics simulations in which the forces necessary to integrate the classical equations of motion are determined in each step by an electronic structure calculations. There have been few examples for such an approach [35–37]. However, in spite of the fact that electronic structure calculations can nowadays performed very efficiently, still there is a significant numerical effort associated with *ab initio* calculations. This effort is so large that in the *ab initio* dynamics simulations addressing molecular adsorption and desorption at surfaces the number of calculated trajectories has been well below 100, a number that is much too low to extract any reliable reaction probabilities.

An alternative approach is the interpolation of the *ab initio* PES by some suitable analytical or numerical scheme. For the six-dimensional quantum dynamical studies of hydrogen dissociation on Pd(100) and Cu(100) discussed in the next section, *ab initio* potential energy surfaces have been fitted to an analytical representations [5, 10, 13, 15, 38].

Most of the corrugation in molecule-surface potential energy surfaces can already be derived from the atom-surface interaction. This observation has been used in corrugation-reducing procedures [39, 40]. First the potential energy surface of both the atomic and the molecular species interacting with a particular surface is determined. From the atomic PES, a three-dimensional reference function is constructed. This function is substracted from the molecular potential energy surface leaving a remaining function that is much smoother than the original potential energy surface and therefore much easier to fit. This method has been successfully used for a continuous representation of the H_2/Pd(111) [39] and the H_2/Ni(111) interaction [40].

However, the parametrization of some set of analytical functions becomes almost impossible if in addition to the molecular degrees of freedom also the substrate degrees of freedom should be included. Then the high-dimensional PES of the molecule interacting with the surface has to be represented as a function of the positions of the substrate atoms. As an intermediate approach, the adjustment of a tight-binding Hamiltonian in order to reproduce the results of *ab initio* total energy calculations has been proposed [41, 42]. A tight-binding method is more time-consuming than an analytical representation since it requires the diagonalization of a matrix. However, due to the fact that the quantum mechanical nature of bonding is taken into account [43] tight-binding schemes need a smaller number of ab initio input points to perform a good interpolation *and* extrapolation [41]. The molecular dynamics simulations of the adsorption of O_2/Pt(111) presented later in this article have been performed using such a scheme.

V. DISSOCIATIVE ADSORPTION AND ASSOCIATIVE DESORPTION OF HYDROGEN AT METAL AND SEMICONDUCTOR SURFACES

The system H_2/Pd has served as the benchmark system for the non-activated dissociative adsorption on surfaces. Figure 3 compares the sticking probability for H_2/Pd(100) as a function of the kinetic energy obtained by molecular beam experiments [44] with the results of six-dimensional quantum calculations based on *ab initio* potential energy surfaces [5, 12]. The experiment shows an initial decrease of the sticking probability as a function of the kinetic energy while at larger kinetic energies the sticking probability slowly rises again.

The decrease of the sticking probability is typical for atomic or molecular adsorption where the molecule adsorbs non-dissociatively. Consequently, it was assumed that the hydrogen molecules do not directly dissociate on Pd(100). They are rather first trapped in a molecular precursor from which they then dissociate [25, 44], and it is the trapping probability into the precursor state that determines the dependence of the sticking probability on the kinetic energy.

However, there is a large mass mismatch between the impinging hydrogen molecule and the palladium substrate. Simple estimates show that the hydrogen molecules do not transfer enough energy to the substrate in order to become trapped at energies above 0.1 eV. Furthermore, the calculated potential energy surface shows no evidence of a metastable precursor state of H_2 at Pd(100). Still the quantum results of the sticking prob-

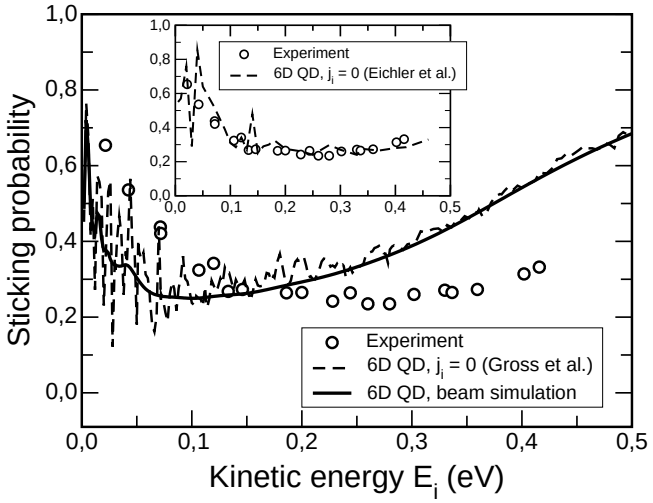

FIG. 3: Sticking probability of H_2/Pd(100) as a function of the initial kinetic energy. Circles: experiment [44], dashed and solid line: theory according to H_2 initially in the ground state and with a thermal distribution appropriate for a molecular beam [5]. The inset shows the theoretical results using an improved *ab initio* potential energy surface [12].

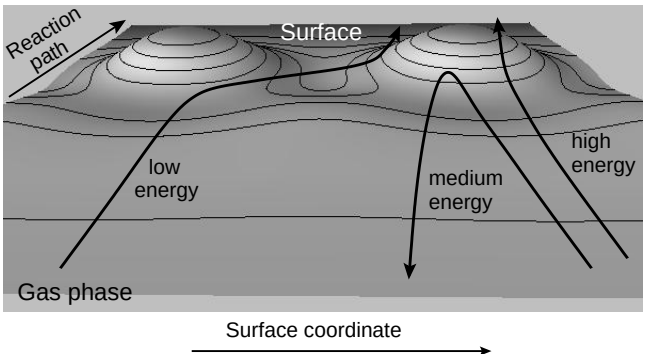

FIG. 4: Illustration of the steering effect on a potential energy surface with a coexistence of purely attractive and repulsive paths towards dissociative adsorption. Three typical trajectories corresponding to the low, medium and high kinetic energy regime are included.

ability [5] are in semi-quantitative agreement with the experiment. As the inset of Fig. 3 demonstrates, with an improved potential energy surface based on more *ab initio* points even quantitative agreement with the experiment can be achieved [12].

The reason for initially decreasing sticking probability is a dynamical process which had been proposed before [45] but whose efficiency had been grossly underestimated: dynamical steering. This process can only be understood if one takes into account the multidimensionality of the PES. The PES of H_2/Pd(100) shows purely attractive paths towards dissociative adsorption, but the majority of reaction paths for different molecular orientations and impact points exhibits energetic barriers hindering the dissociation.

At very low kinetic energies the particles are so slow that they can be very efficiently steered to a favorable configuration for dissociation. This leads to a very high dissociation probability. Since this mechanism becomes less effective at higher kinetic energies, the reaction probability decreases. This scenario is illustrated in Fig. 4. A cut through the six-dimensional potential energy surface of H_2/Pd(100) is plotted along the reaction path coordinate and one surface coordinate. The reaction path coordinate connects the molecule in the gas phase with the dissociated molecule on the surface. There is one purely attractive path in the center which corresponds to the dissociation at the hollow-bridge-hollow configuration indicated in Fig. 2a while the path directly over the maximum barrier in Fig. 4 represents the dissociation above the top site.

Three typical trajectories are included in Fig. 4. The low and medium energy trajectories are related to each other by the mirror symmetry along the surface coordinate. They are supposed to have the same initial conditions except for the initial kinetic energy. Both energies are too small to allow a direct crossing of the barrier the particles are directed at. However, at the low kinetic energy the forces acting on the incoming particle can redirect it so that it follows a path that leads to the purely attractive region of the PES. At the medium energy, of course the same forces act on the incoming particle. But now it is too fast to be steered significantly. It is reflected at the repulsive part of the potential and scattered back into the gas phase. This suppression of the steering effect for increasing kinetic energy leads to the initial decrease of the sticking probability in Fig. 3. If the energy is further increased, then the particles will eventually have enough kinetic energy to directly cross barriers, as the high-energy trajectory illustrates in Fig. 4. This leads to the rise of the sticking probability at high kinetic energies.

In general, the reactive trajectories are not always as simple as illustrated in Fig. 4. In particular in the low-energy regime, impinging particles may not directly either adsorb or scatter. They can convert part of their initial kinetic energy into internal and lateral degrees of freedom, so that the particles do not have enough kinetic energy to escape back into the gas phase, but also do not come to rest at the surface. This leads to a dynamical trapping of the particles [8, 9, 46] which will be discussed in detail below.

The steering effect is strongly suppressed if the impinging molecules are rapidly rotating because molecules with a high angular momentum will rotate out of a favorable orientation towards dissociative adsorption during the time it takes to break the molecular bond. The dependence of the sticking probability on the initial rotational state was proposed as a property that can be used to distinguish between the steering and the precursor mechanism [47]. Molecular adsorption into a weak precursor state should be relatively independent of the

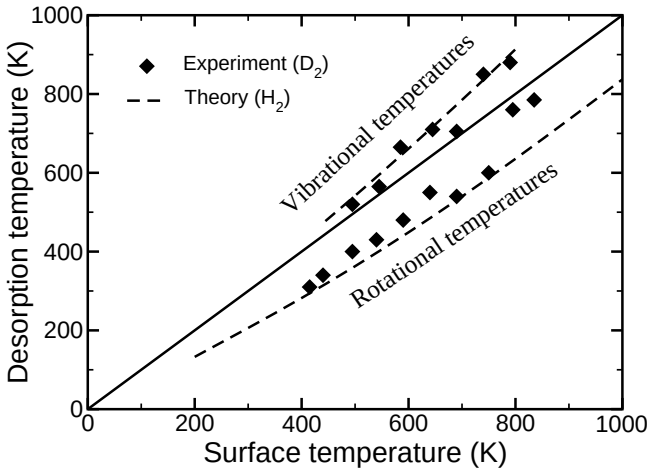

FIG. 5: Vibrational and rotational temperatures of hydrogen desorbing from Pd(100) as a function of the surface temperature. The experimental results have been determined by tunable vacuum ultraviolet laser ionization spectroscopy for D_2 while the theoretical results have been derived from six-dimensional quantum calculations for H_2 (after [50]).

rotational motion. This rotational hindering of the steering effect has actually been confirmed for H_2/Pd(111) [48, 49]. By seeding techniques the translational energy of a H_2 beam has been changed in a nozzle experiment without altering the rotational population of the beam. The rotationally hot beams showed a much smaller sticking probability than rotationally cold beams [48, 49].

The influence of internal molecular degrees of freedom on the dissociation process can also be probed by studying the time-reversed process of dissociative adsorption, associative desorption, using the concept of microscopic reversibility or detailed balance [51, 52]. In Fig. 5, so-called rotational temperatures in desorption are plotted. They correspond to the mean rotational energy in desorption via $T_{\rm rot} = \langle E_{\rm rot} \rangle / k_B$. According to the principle of detailed balance, the suppression of the sticking probability by the rotational hindering should be reflected by a population of rotational excited states in desorption which is lower than expected for molecules in thermal equilibrium with the surface temperature. The experimental results have been obtained by tunable vacuum ultraviolet laser ionization spectroscopy for D_2 [50]. Deuterium is often used in desorption experiments because of the unavoidable H_2 background in the vacuum chambers. The calculations, on the other hand, are done for H_2 because of the much smaller computational effort for light hydrogen in quantum methods. Still both experiment and theory agree well as far as the so-called rotational cooling is concerned, thus confirming the rotational hindering.

In Fig. 5, additionally the calculated and measured vibrational temperatures [50] are plotted. In contrast to the rotational cooling, there is vibrational heating indicating that there should be enhanced dissociation for vibrating hydrogen molecules on Pd(100). Vibrationally enhanced dissociation has been known for years in the gas phase dynamics community [53]. Usually it is associated with strongly curved reaction paths in activated systems [4]. However, the most favorable path towards dissociative adsorption in the system H_2/Pd(100) is purely attractive and has a rather small curvature (see Fig. 2a). Therefore one would not expect any substantial influence of the vibrational state of H_2 on the sticking probability.

In fact, the vibrational effects in the system H_2/Pd(100) are also present in adiabatic calculations in which the vibrational state of the molecule is kept fixed so that no vibrational transitions are allowed [54]. A detailed analysis showed that the vibrational effects in the dissociation of H_2/Pd(100) are caused by the strong lowering of the H-H vibrational frequency during the adsorption and the multi-dimensionality of the relevant phase space with its broad distribution of barrier heights. This can be understood from the fact that the vibrational motion corresponds to the fastest degree of freedom in this system so that the vibrational energy acts as an adiabatic invariant. The higher the vibrational energy, the stronger the effect of the lowering of the vibrational frequency. Therefore vibrationally excited molecules experience a potential energy surface with effectively lower barriers than molecules in the vibrational ground state causing vibrationally enhanced dissociation in adsorption and vibrational heating in desorption.

Earlier experiments showed a vibrational overpopulation of the first excited vibrational state in desorption that was higher than the vibrational ground-state population by a factor of nine [55]. This result was later questioned on the basis of the quantum calculations which only found an overpopulation by a factor of 2.5 [54]. When the experiments were repeated, the theoretical predictions were confirmed [50], as Fig. 5 demonstrates. This indicates that in the field of surface science theory has reached a level of reliability that makes predictions possible and allows a fruitful and close collaboration with experiment.

The reliability of high-dimensional quantum calculations based on *ab initio* potential energy surfaces is also demonstrated in Fig. 6, where the sticking probability of H_2/Cu(100) obtained by six-dimensional wave packet calculations [32] is compared to experimental results derived from an analysis of adsorption and desorption experiments [27]. The measured experimental sticking probabilities and, via the principle of *detailed balance*, also desorption distributions had been fitted to the following analytical form of the vibrationally resolved sticking probability as a function of the kinetic energy:

$$S_v(E) = \frac{A}{2}\left\{1 + \tanh\left(\frac{E - E_0(v)}{W(v)}\right)\right\} \qquad (10)$$

The agreement between theory and experiment in Fig. 6 is very satisfactory except for the fact that the experimentally derived sticking probabilities level off at a value of about 0.4 while the calculated sticking probabilities

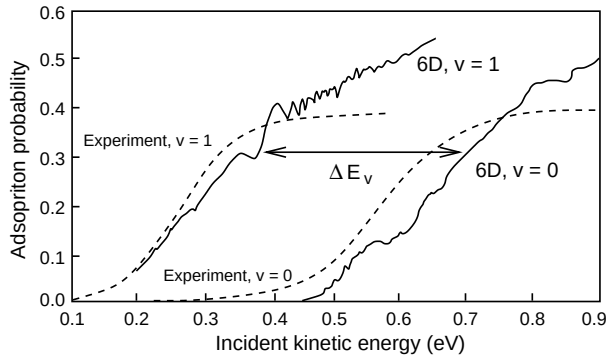

FIG. 6: Dissociative adsorption probability of H_2 on Cu(100) as a function of the incident kinetic energy determined by six-dimensional quantum wave-packet calculations for molecules initially in the vibrational ground state and first excited state, respectively [32]. For the vibrational ground state, the calculations are compared to experimental results derived from an analysis of adsorption and desorption experiments [27].

are still rising. However, this should be no serious concern. Molecular beam experiments of H_2 typically only reach kinetic energies of up to 0.5 eV [33, 34], only for D_2 kinetic energies of up to 0.8 eV are possible through seeding with H_2 [28]. Hence the experimental data of H_2 in Fig. 6 for kinetic energies above 0.5 eV are derived from thermal desorption experiments in which the higher energy contributions are exponentially suppressed through the Boltzmann factor. Therefore there is a large uncertainty about the high-energy regime.

The onset of the sticking probability at approximately 0.5 eV for H_2 molecules initially in the vibrational ground state is given by the minimum energy barrier including zero-point effects. The zero-point effects arise from the quantization of the molecular levels due to the localisation of the wave function in the degrees of freedom perpendicular to the reaction path at the minimum barrier position. In a high-barrier system such as H_2/Cu, steering effects only play a minor role in the adsorption dynamics. The rise in the sticking probability is rather determined by the distribution of the barrier heights for dissociative adsorption in the multidimensional potential energy surface [31]. Thus sticking can be understood in terms of the region of the surface that classically is available to dissociation which is the basis of the so-called *hole model* [56].

As Fig. 6 demonstrates, in the system H_2/Cu the sticking probability is significantly enhanced if the impinging molecules are initially vibrationally excited. In order to quantify the effect the *vibrational efficacy* is introduced. It is defined as

$$\chi = \frac{\Delta E_v}{\hbar\omega_{\rm vib}}, \tag{11}$$

where ΔE_v is the energetic shift between the sticking curves for molecules in the vibrationally ground and first-excited state. In Fig. 6 we have indicated the energy shift which is of course not uniquely defined since the two sticking curves are not really parallel to each other. This shift is approximately 0.3 eV so that for the vibrational frequency of H_2, $\hbar\omega_{\rm vib} = 0.516$ eV, the vibrational efficacy is $\chi \approx 0.6$. This means that 60% of the vibrational energy is used to overcome the barrier for dissociative adsorption.

In contrast to H_2/Pd, the vibrational effects in the adsorption of H_2/Cu(100) are mainly caused by the curved reaction path. The basic mechanism can be discussed within a two-dimensional elbow plot shown in Fig. 2b. The PES corresponds to a so-called late barrier system which refers to the fact that the barrier is located after the curved region of PES. If the molecule is already initially vibrating, i.e., if it is oscillating back and forth in the d-direction, then the vibrational energy can be very efficiently used "to make it around the curve" and enter the dissociation channel. Nevertheless, adiabatic effects as just discussed in the context of the hydrogen dissociation on Pd(100) also contribute to the vibrational effects for H_2/Cu(100).

Once a six-dimensional PES is available, sticking and scattering probabilities as a function of the incident angle and the internal state of the molecule can be evaluated [57, 58]. In a combined experimental and theoretical study the rovibrationally inelastic scattering of H_2 molecules initially in the $(v = 1, j = 1)$ from Cu(100) has been addressed [59]. Theory and experiment were in good agreement for the survival probability, i.e., the probability for rovibrationally elastic scattering. However, as far as the rovibrationally inelastic scattering is concerned, the theory has overestimated the probabilities for channels that could be detected experimentally. The reasons for the discrepancies have not been clarified, but it could well be that either inaccuracies inherent in the DFT or in the fitting procedure of the PES are responsible [59]. In particular, there is still an intrinsic inaccuracy of the GGA functionals [24] which might be also relevant for the H_2/Cu system [60]. These problems that still exist in the framework of DFT calculations should be considered when the reliability of *ab initio* potential energy surfaces is assessed.

As already mentioned, in the case of semiconductor surfaces there is often a strong surface rearrangement upon adsorption due to the covalent bonding of the semiconductor substrate. The benchmark system for the study of the adsorption and desorption dynamics at semiconductor surfaces is the interaction of hydrogen with silicon surfaces [2, 61]. Apart from the fundamental interest, this system is also of strong technological relevance for the growth and passivation of semiconductor devices.

It is a well-studied system [2, 61], but still it is discussed very controversely, as far as experiment [62–67] as well as theory is concerned [14, 36, 37, 68–73]. This debate was fueled by the so-called barrier puzle: While the sticking coefficient of molecular hydrogen on Si surfaces is very small [67, 74] indicating a high barrier to adsorption, the low mean kinetic energy of desorbed molecules

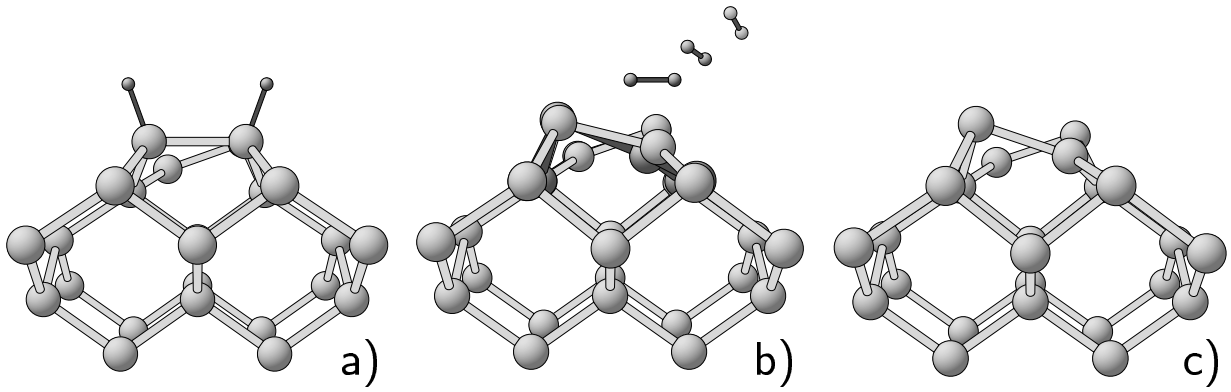

FIG. 7: a) Hydrogen covered Si (100) surface (monohydride). b) Snapshots of a trajectory of D_2 desorbing from Si (100) starting at the transition state with the Si atoms initial at rest [37]. The dark Si atoms correspond to the Si positions after the desorption event. c) Clean anti-buckled Si (100) surface [37].

[62] suggests a small adsorption barrier. One of the debated issues is the role of the surface rearrangement of the silicon substrate degrees of freedom upon the adsorption and desorption of hydrogen which was believed to be the cause of the barrier puzzle [62, 68]: The hydrogen molecules impinging on the Si substrate from the gas phase typically encounter a Si configuration which is unfavorable for dissociation, while desorbing hydrogen molecules leave the surface from a rearranged Si configuration with a low barrier.

The Si(100) surface shows a antibuckled $p(2 \times 2)$ reconstruction which is illustrated in Fig. 7c. As far as the hydrogen dissociation is concerned, there are two possible pathways on clean Si(100): the *intradimer* pathway where the hydrogen atoms of the dissociating molecule end up on both ends of a dimer, and the *interdimer* pathway where the H-H bond is oriented perpendicular to the Si dimers and the hydrogen atoms adsorb at two neighboring dimers. An earlier study suggested that the adsorption barrier of the interdimer pathway is approximately 0.3 eV higher than the intradimer barrier [75]. Therefore, most DFT slab studies first focused on the intradimer pathway [37, 76, 77]. Upon adsorption of H_2 on a Si dimer, the buckling of the dimer (Fig. 7c) is lifted and the dimer becomes symmetric in the monohydride phase (Fig. 7a). This strong surface rearrangement was considered as a possible candidate responsible for the barrier puzzle [68, 76, 77]. *Ab initio* molecular dynamics simulations were performed in order to determine the energy distribution of hydrogen molecules desorbing from Si(100) [37]. Snapshots of one of the forty calculated trajectories are shown in Fig. 7b. The dark Si atoms correspond to the relaxation of the Si lattice after the desorption event. Approximately 0.1 eV of the potential energy at the transition state is transfered to vibrations of the Si lattice. The simulations reproduced the vibrational heating and the rotational cooling observed in the desorption experiments [61]. However, the kinetic energy in desorption was still much larger in the *ab initio* molecular dynamics runs than in the experiment [62]. This is due to the fact that the elastic energy of the surface frozen in the transition state configuration is only about 0.15 eV [77] which is too little in order to take up the energy of the transition state.

Later the barrier puzzle was resolved in a close collaboration between experiment and electronic structure calculations. It turned out that it is not sufficient to just consider the H_2 dissociation on clean Si(100). Instead it was realized that it is very important to take into account the exact surface structure and surface coverage in the determination of the adsorption/desorption barriers [64, 72]. At surface imperfections such as steps the reactivity of a surface can be extremely modified. It was found experimentally on vicinal Si(100) surfaces that the sticking coefficient at steps is up to six orders of magnitude higher than on the flat terraces [71]. This finding was supported by DFT studies which showed that nonactivated dissociation of H_2 on the so-called rebonded D_B steps on Si(100) is possible [71, 78], while on the flat Si(100) terraces the dissociative adsorption is hindered by a barrier of 0.4 eV [37].

Since the electronic structure of the dangling bonds is perturbed in a similar way by both steps and adsorbates [72], adsorbates can have a similar effect on the dissociation probability as steps. Recent scanning tunneling microscope (STM) experiments showed that predosing the Si(100) surface by *atomic* hydrogen creates active sites at which the H_2 adsorption is considerably facilitated [79]. Actually the predosing of atomic hydrogen makes the adsorption of H_2 in an interdimer configuration possible. This renewed the interest in the theoretical study of the interdimer pathway. The interdimer pathway was revisited by DFT-GGA calculations [72] which in fact found that its barrier is *smaller* than the barrier along the intradimer pathway. The discrepancy to the former calculations [75] was attributed to the fact

that a different transition state geometry had been considered. The DFT-GGA calculations further confirmed that on hydrogen-precovered Si(100) highly reactive sites exist at which H_2 can spontaneously dissociate.

Now a consistent picture of the adsorption/desorption of H_2/Si(100) has emerged. On the one hand, H_2 molecules can desorb from hydrogen-covered Si(100) at full coverage without being accelerated towards the gas phase which explains the low kinetic energy measured in desorption experiments [62, 80]. On the other hand, in adsorption experiments at low coverages, this dissociation path without a barrier is not present at clean Si(100) which leads to the small observed sticking probability. At intermediate coverages, both activated as well as non-activated adsorption paths are present leading to a crossover from activated dissociation dynamics to non-activated dissociation dynamics.

VI. MOLECULAR TRAPPING OF OXYGEN AT METAL SURFACES

The adsorption of oxygen on platinum is of great technological relevance since it represents one of the fundamental microscopic reaction steps occuring in the car-exhaust catalyst. This fact has motivated, in addition to the fundamental interest, a large number of studies of the interaction of O_2 with Pt(111) [81–88] so that it has become one of the best studied systems in surface science.

I will first summarize the experimental findings with respect to the adsorption of O_2 on Pt(111). At surface temperatures below 100 K, three molecular O_2 adsorption states have been identified. Below 30 K, a weakly bound physisorbed species exists [82, 88]. Up to 100 K, two different kinds of molecularly chemisorbed states are found [89, 90] which have been characterized as peroxo-like (O_2^{-2}) and superoxo-like (O_2^{-}), respectively. This assignment of the chemisorbed molecular states has been confirmed by total-energy calculations [91, 92] using density functional theory (DFT) within the generalized gradient approximation (GGA) [23]. According to these calculations, the superoxo-like O_2 species that still has a magnetic moment corresponds to an O_2 molecule adsorbed over the bridge position with the two O atoms oriented towards the adjacent Pt atoms in a so-called top-bridge-top (t-b-t) configuration. The binding energy according to the GGA-DFT calculations is about 0.7 eV.

The non-magnetic peroxo species has been identified as O_2 molecules adsorbed in a slightly tilted bridge-hollow-top configuration above the threefold hollow sites. The fcc and hcp hollow sites are energetically almost degenerate with binding energies of 0.7 and 0.6 eV, respectively. The O_2 physisorption state could not be identified in the DFT calculation since the current exchange-correlation functional do not reproduce the long-range van der Waals attraction.

Figure 8 shows the sticking probability of O_2/Pt(111)

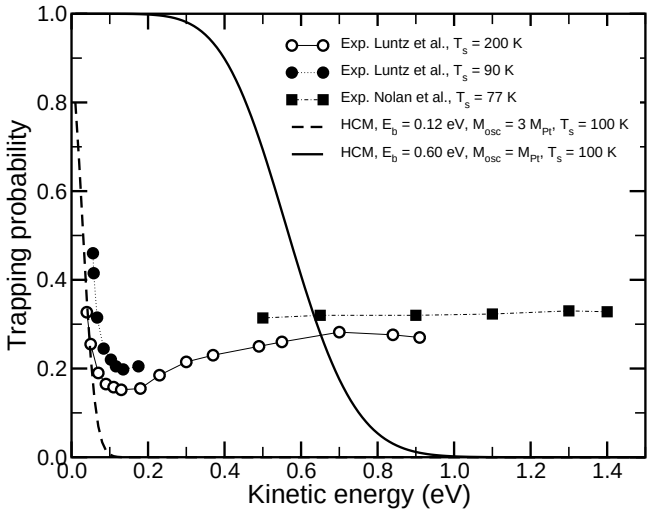

FIG. 8: Trapping probability of O_2/Pt(111) as a function of the kinetic energy for normal incidence. Results of molecular beam experiments for surface temperatures of 90 K and 200 K (Luntz *et al.* [81]) and 77 K (Nolan *et al.* [87]) are compared to simulations in the hard-cube model (HCM).

as a function of the kinetic energy as measured in molecular beam experiments [81, 87]. First there is a strong decrease [81], and then after passing a minimum at approximately 0.15 eV the sticking probability levels off at a value of about 0.3 [81, 87]. Furthermore, molecular beam experiments yielded the rather surprising result that oxygen molecules do not dissociate at cold Pt surfaces below 100 K [83, 86, 87], even at the highest accessible kinetic energies of 1.4 eV which are much greater than the dissociation barrier.

The experimental findings have been rationalized using an one-dimensional representation of the potential energy surface that is plotted in Fig. 9 [87]. The strong initial decrease of the sticking probability has been attributed to the trapping of O_2 in the physisorption state [83]. Since the well depth of physisorption states is usually rather small, the trapping probability into such shallow wells decreases rather rapidly as a function of the incident kinetic energy. Using the hard-cube model (HCM, eq. (3)), i.e., treating the O_2 molecule as a point-like object impinging on a flat, structureless surface, the initial decrease could be reproduced assuming a physisorption well depth of 120 meV [83]. The results of this hard-cube analysis are also included in Fig. 8. In addition, the HCM sticking probability for trapping into a chemisorption well of depth 0.6 eV is plotted. This curve does not resemble the experimentally determined sticking probablities at all, so that direct trapping into any chemisorption state seemed to be excluded according to the hard-cube model.

The increase of the sticking probability at higher kinetic energies was attributed to a direct access of the chemisorbed molecular states [81, 83, 86, 87], which is also sketched in Fig. 9. Now, such an one-dimensional sketch of the potential energy surface along some suit-

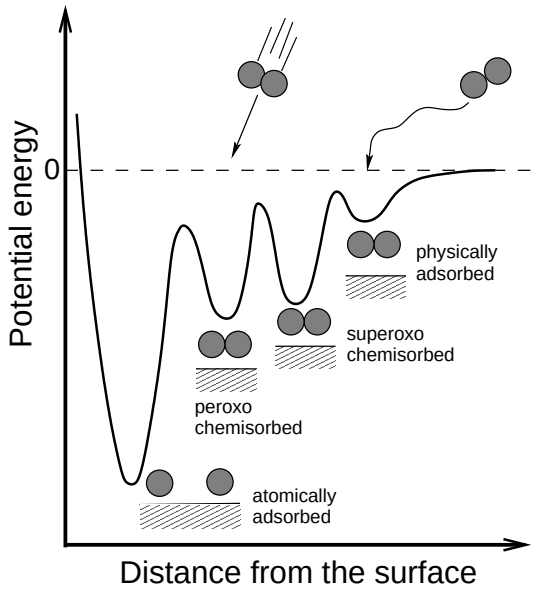

FIG. 9: Schematic presentation of the one-dimensional potential energy surface for oxygen adsorption on Pt(111) as derived from experiment (after [87]).

able reaction coordinate is certainly very helpful for a compact presentation of the energetics of reaction intermediates and products. Furthermore, it can be used as a basis for a *kinetic* modelling of a reaction. However, in order to understand the microscopic *dynamics* of a reaction, such an one-dimensional illustration of the potential energy surface is not really helpful, in fact it can even be misleading. Instead of providing an explanation for the observed results it rather creates new questions. Why should the O_2 molecule approching the Pt(111) surface be trapped in one of the molecular adsorption wells instead of directly propagating towards the dissociation channel? The dissociation barrier derived from a kinetic interpretation of the experimental results is below the molecular vacuum level [87], hence the molecule could in principle directly access the dissociation channel if there is no energy dissipation along the reaction path.

In order to shed light on the mechanism of O_2 sticking on Pt(111) a microscopic simulation of the adsorption dynamics is called for. However, such a simulation represents a great challenge compared to, e.g., the dynamical simulation of hydrogen dissociation at metal surfaces discussed in the previous section where the substrate degrees of freedom can usually safely be neglected [2, 3]. For the theoretical description of the adsorption of O_2/Pt(111), on the one hand a realistic potential energy surface (PES) is needed that reliably describes both the molecular as well as the dissociative adsorption channels. On the other hand, molecular trapping processes can only be reproduced if the energy dissipation to the platinum substrate is properly taken into account. Direct *ab initio* molecular dynamics simulations represent a scheme that meets these requirements. But as we already saw in the last section, the computational effort of running *ab initio* trajectories is still very high. This prevents the evaluation of a sufficient number of trajectories necessary for a reliable determination of reaction or sticking probabilities [2, 37]. Using empirical classical potentials, almost arbitrarily many trajectories could be computed. However, up to now no accurate scheme has been established for the generation of classical potentials that are able to reliably reproduce the potential energy surface of a reaction on a surface as a function of the position of the substrate atoms.

Thus an intermediate method is required that is less time-consuming than an *ab initio* approach but still properly describes the quantum nature of bond breaking and bond making at surfaces. The tight-binding (TB) method represents such a compromise. The evaluation of the tight-binding Hamiltonian still requires the diagonalization of a matrix. Nevertheless, the tight-binding calculations are about three orders of magnitude faster than the DFT calculations making the evaluation of hundreds of trajectories possible. Originally tight-binding was only formulated to yield band-structure energies [93]. Later the method was extended to allow the evaluation of total energies [94]. Such an extension can be validated on the basis of density-functional theory [95] (see Ref. [43] for a review). In tight-binding, the exact many-body Hamiltonian is replaced by parametrized Hamiltonian matrix elements of the effective one-particle Hamiltonian in an atomic-like basis set. The atomic-like basis functions are usually not considered explicitly, but the matrix elements are assumed to have the same symmetry properties as matrix elements between atomic states.

The tight-binding matrix elements are often determined empirically (see, e.g., [96]), but there are recent TB formulations in which the matrix elements are derived from first-principles electronic structure calculations [41, 42, 97]. One of these *ab initio* derived schemes is the so-called NRL tight binding method developped at the Naval Research Lab [42]. Unlike other tight-binding methods [43, 97, 98], this TB scheme does not include a pair-potential term. Instead, the total energy of the system is just represented by the sum of eigenvalues that are shifted depending on the structure and volume. The method also contains environment-dependent on-site terms that account for the effects of the local neighborhood on each atom [42].

The NRL tight-binding method has been used to address the adsorption of O_2 on Pt(111) [99]. The Pt-Pt interactions were taken from a large data base of TB parameter for the elements which are posted on the world wide web [100]. These parameters were obtained from a fit to DFT bulk calculations. Still, it has been demonstrated that the pure Pt surface is also well-described by this parametrization [42]. For the Pt-O and the O-O TB parameters a new fit had to be performed. They were adjusted in order to reproduce the GGA-DFT results of the O_2/Pt(111) potential energy surface [91, 92]. The root mean square error of the fit is below 0.1 eV [41] which is

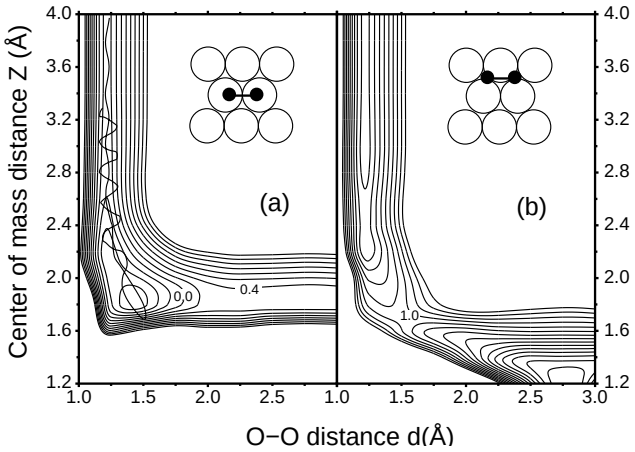

FIG. 10: Potential energy surface of the dissociation of O_2/Pt(111) determined by the *ab initio* derived tight-binding Hamiltonian. The coordinates in the figure are the O_2 center-of-mass distance from the surface Z and the O-O interatomic distance d. The configurations of the remaining O_2 degrees of freedom are illustrated in the insets. The contour spacing is 0.2 eV per O_2 molecule. In (a) a trajectory of an O_2 molecule with an initial kinetic energy of 0.6 eV scattered at Pt(111) is also plotted.

in the range of the error of the GGA-DFT calculations. The spin state of the oxygen molecule was not explicitly considered in the TB Hamiltonian. This corresponds to the assumption that the electron spins follow the motion of the nuclei adiabatically and remain in their ground state.

The potential energy surface of O_2/Pt(111) obtained from the tight-binding Hamiltonian is illustrated in Fig. 10 where two representative elbow plots are shown. These plots might be compared with the corresponding original DFT contour graphs shown in Ref. [92]. Panel (a) presents the elbow plot of the superoxo molecular precursor state located above the bridge site. The access from the gas phase is non-activated, i.e. it is not hindered by any barrier. The peroxo states above the threefold hollow sites (not shown) which are energetically almost degenerate with the superoxo state [91] can also be directly accessed from the gas phase.

The O_2/Pt(111) PES is in fact strongly corrugated, i.e. the interaction depends significantly on the lateral position of the O_2 molecule. If the molecule is only shifted by about 1 Å in lateral direction from the superoxo configuration, the nature of the interaction is changed from attraction towards the molecular precursor to strong repulsion with a barrier towards dissociation of almost 1 eV (Fig. 10b). Above the top position the barrier for dissociation even increases to 1.3 eV for an O_2 molecule with its axis parallel to the surface [92]. For a molecule approaching the surface in an upright fashion the PES is purely repulsive. Consequently, O_2 can not adsorb and dissociate on Pt(111) with its axis being perpendicular to the surface which means that the PES exhibits a high polar anisotropy. However, also rotations with the O_2 axis parallel to the surface are strongly hindered for example at the threefold hollow positions [92]. In fact, the majority of adsorption channels are hindered by barriers; direct non-activated access of the molecular precursor states is possible for only a small fraction of initial conditions.

Using the NRL-TB parametrization, molecular dynamics simulations of the adsorption of O_2/Pt(111) have been performed with the tight-binding molecular dynamics code TBMD [101] using a five-layer slab to model the Pt substrate. The chosen time step was 1 fs, and the bottom layer of the Pt slab was kept fixed while all other Pt atoms were allowed to move in order to allow energy transfer from the impinging molecule to the substrate. No zero-point energies were taken into account in the initial conditions. This has been shown to be appropriate for the classical simulation in the system H_2/Pd(100) where the decrease in the molecular vibrational zero-point energy is compensated for by the building up of zero-point energies in the other molecular degrees of freedom [8, 15]. There can still be quantitative differences between quantum calculations and classical and so-called quasiclassical simulations, in which zero-point energies are taken into account in the initial conditions [16], the qualitative trends, however, are most often reproduced.

In classical molecular dynamics simulations, reaction probabilities in general are determined by averaging over the results of many trajectories whose initial conditions are usually picked at random. The statistical uncertainty of the calculated reaction probabilities is then given by $1/\sqrt{N}$, where N is the number of calculated trajectories. This also means that it is computationally very demanding to determine small reaction probabilities since any calculated probability below $1/\sqrt{N}$ is statistically not significant.

Since the TBMD calculations still require the diagonalization of matrices whose dimension is given by the considered electronic states, there is still some computational effort associated with these simulations [102]. The O_2/Pt(111) sticking probabilities have been determined by averaging over 150 trajectories for each energy so that there is a statistical error of $1/\sqrt{150} \approx 0.07$ associated with the calculated probabilities. Although this statistical uncertainty is still rather large, it allows to identify qualitative trends in the system O_2/Pt(111) where the measured sticking probabilities are all larger than 0.15 (see Fig. 8).

Furthermore, a criterium has to be given that specifies the trajectories which are considered to represent trapping events. It should be noted here that there is no unambiguous definition of the sticking probability because for surfaces with non-zero temperature every adsorbed particle will sooner or later desorb again. Hence the sticking probability depends on the time-scale of the required residence time on the surface. Usually this does not cause problems for any practical purposes. A particle that has equilibrated at the surface might be safely con-

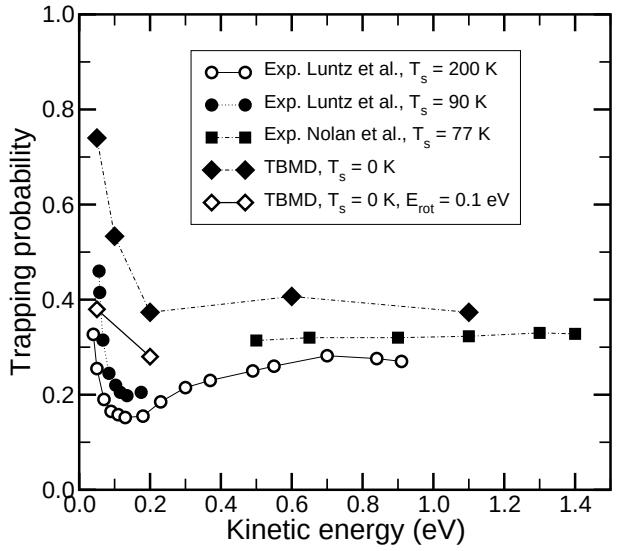

FIG. 11: Trapping probability of O_2/Pt(111) as a function of the kinetic energy for normal incidence. Results of molecular beam experiments for surface temperatures of 90 K and 200 K (Luntz *et al.* [81]) and 77 K (Nolan *et al.* [87]) are compared to tight-binding molecular dynamics simulations for the surface initially at rest ($T_s = 0$ K).

sidered as being trapped. To be specific, in the TBMD simulations a trajectory was considered to correspond to a trapping event when the molecule stayed for more than 2 ps at the surface; furthermore, at a surface temperature of $T_s = 0$ K a particle was already be considered as being trapped if it had transferred more than its initial energy to the surface.

In order to simulate the energy transfer to the substrate, either the considered system has to be large enough to take up the energy without any feedback artifacts, or it has to be coupled to a heat bath to allow for dissipation. Typically in molecular dynamics simulations the heat bath is modeled either by the *generalized Langevin equation* approach [103] or by the *Nosé thermostat* [104, 105]. The TBMD simulations were mainly performed within the microcanonical ensemble. The surface unit cells, $c(4 \times 2)(111)$ for the lower energies and $c(4 \times 4)(111)$ for energies above 0.5 eV, turned out to be sufficiently large which was checked by coupling the bottom layer of the slab to a heat bath via the generalized Langevin equation.

Figure 11 presents the calculated sticking probabilities of O_2/Pt(111) as a function of the kinetic energy for normal incidence with the surface initially at rest, i.e. at a surface temperature of $T_s = 0$ K. Quantitatively, the TBMD results are larger than the molecular beam data [81, 87]. This might be attributed to the fact that the PW91-GGA functional [23] used in the DFT calculations overestimates the binding energies of the molecular adsorption state by 0.2–0.3 eV [91, 92, 106] compared to the experiment [89, 107] so that the PES is too attractive. Still the qualitative trend found in the experiments is well-reproduced by the TBMD simulations. Since there is no physisorption well present in the used PES, the strong initial decrease of the sticking probability as a function of the kinetic energy can not be caused by trapping into the physisorbed precursor state.

In order to determine the microscopic trapping mechanism, a detailed analysis of the trajectories has been performed. This analysis showed that at kinetic energies below 0.2 eV all molecules that enter the molecular chemisorption wells get in fact trapped. Thus it is *not* the energy transfer to the substrate *per se* that determines the sticking probability at low kinetic energies but rather the probability to enter the attractive adsorption channels. This suggests that it is the suppression of the *steering mechanism* as in the system H_2/Pd(100) that is responsible for the minimum of the sticking probability at medium energies.

This hypothesis is confirmed by the analysis of the trajectories. In Fig. 12 snapshots of TBMD trajectories of an O_2 molecule impinging on a Pt(111) surface with kinetic energies of 0.05 eV and 0.20 eV are shown. Except for the kinetic energgy both trajectories had the same initial conditions. This figure corresponds to the real-space analogue of the schematic illustration of the steering mechanism shown in Fig. 4. The molecule approaches the surface in a canted configuration in which it can not adsorb on the surface. At the low energy, the forces acting on the molecule reorient the molecule into a parallel configuration. In fact there is even some *oversteering*, as the panel for $t = 200$ fs shows, i.e. the molecule rotates out of the favorable parallel orientation. However, at $t = 350$ fs the molecule is oriented parallel again, and at $t = 1000$ fs it is adsorbed in a slightly tilted configuration in the peroxo chemisorption state above a threefold hollow position.

At the higher kinetic energy, of course the same forces act upon the molecule. But now the molecule is too fast to become significantly reoriented before it hits the repulsive wall of the potential at $t = 50$ fs. When the molecule reaches the surface in the tilted configuration, it starts quickly rotating in a flip-flop motion until the other end hits the surface. The molecule is then scattered back into the gas phase rotationally excited (which can not been infered from the panel at $t = 300$ fs).

In order to further confirm that the steering mechanism is indeed operative at low kinetic energies, the sticking probability for initially rotating molecules at $E_{\rm kin} = 0.05$ eV has been determined as well. The sticking probability is strongly suppressed by the additional rotational motion, as Fig. 11 shows. This rotational hindering is a strong signature of the steering mechanism [47]. An initial rotational energy of $E_{\rm rot} = 0.1$ eV also causes a rotational hindering of the adsorption at $E_{\rm kin} = 0.2$ eV (see Fig. 11). The molecules in the molecular beam experiments are in fact not in their rotational ground state, but they are also rotating with a mean kinetic energy that depends on the nozzle temperature and the particular molecular species. A rotational energy of 0.1 eV

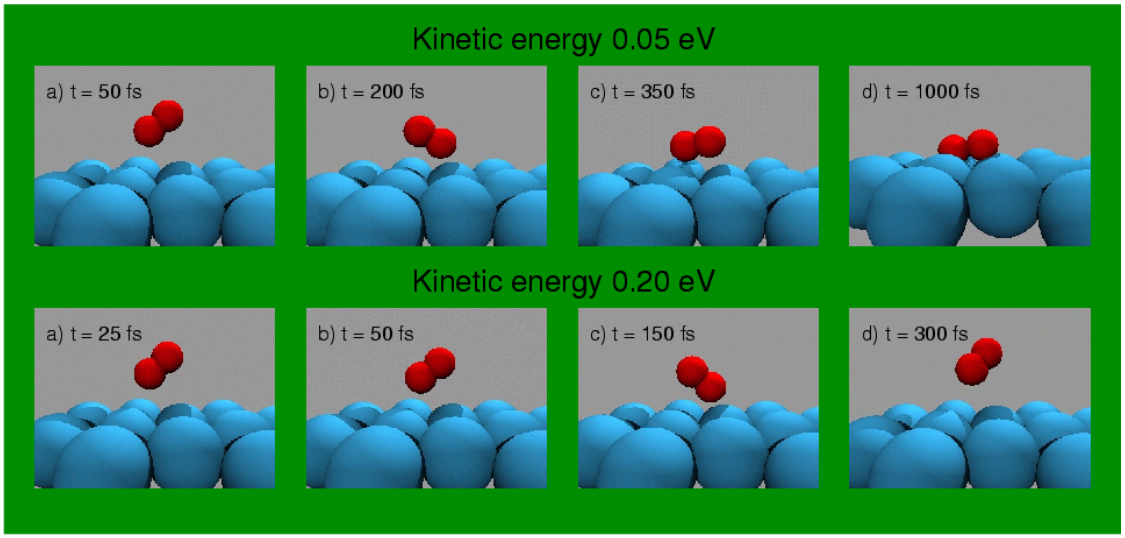

FIG. 12: Snapshots of TBMD trajectories of an O_2 molecule impinging on a Pt(111) surface with the same initial conditions except for the kinetic energy of 0.05 eV and 0.20 eV, respectively.

seems to be reasonable for a beam of O_2 molecules with $E_{\mathrm{kin}} = 0.2$ eV [108]. Hence by taking into account the rotational motion of the molecules, the quantitative difference between theory and experiment is significantly reduced.

Since no physisorption well is present, the question has to be considered how the inclusion of a physisorption state would alter the trapping dynamics. Physisorption wells are created by a combination of the attractive van der Waals interaction with Pauli repulsion caused by the overlap of molecular and substrate wave functions. While the former effect is not reproduced by the DFT calculation, the repulsion due to wave function overlap is well described by present DFT functionals. Hence the calculated PES would only become more attractive if van der Waals forces were correctly included. For a more quantitative description of the trapping process at kinetic energies below 0.05 eV certainly the physisorption channel has to be included.

However, the important point is that the simulations clearly demonstrate that a physisorption state is not needed in order to reproduce the strong initial decrease of the trapping probability at low energies. The van der Waals attraction is rather independent of the lateral position along the surface since it is a long-range effect. Therefore its inclusion would anyhow not qualitatively change the adsorption dynamics at kinetic energies above 80 meV at which there is almost no trapping into the physisorption well (see Ref. [83]).

At higher energies, the leveling off of the measured sticking probabilities is reproduced by the calculations. Such a behavior is not typical for molecular dynamics simulation which usually yield a monotonously decreasing sticking probability for molecular trapping processes. Again, an analysis of the trajectories sheds light on the underlying microscopic mechanism. In Fig. 13, snapshots and the energy redistribution of a typical O_2 trajectory with a kinetic energy of 1.1 eV are plotted.

At such a high energy, even molecules with unfavorable initial conditions can get close to the surface. However, there is a negligible probability that in the first collision the high energy particles will transfer enough energy to the surface to remain trapped, as the analysis using the hard-cube model confirms (see Fig. 8). In the case of Fig. 13, the molecules hits the surface in a tilted configuration ($t = 50$ fs). Only very little energy is transfered to the platinum substrate.

However, the molecule impinging in the tilted orientation starts rotating very rapidly upon the impact ($t = 115$ fs). In fact, more than 1 eV is transfered into this rotational motion. In addition, the molecule also starts to vibrate. The snapshot at $t = 500$ fs depicts the molecule in an elongated situation. The energy stored in the rotational and vibrational motion is not available for a direct escape from the adsorption well. Although the molecule is scattered back after the first impact, it is not able to leave the adsorption well; consequently, it becomes dynamically trapped for a while [8, 9]. While being trapped, the molecule hits the surface several times and transfers successively more and more energy to the substrate until it equilibrates. As Fig. 13 shows, at about 1.3 ps after the first collision the O_2 molecule has become accommodated at the Pt(111) surface for this particular trajectory in the superoxo state in the t-b-t configuration, as the snapshot at $t = 1700$ fs illustrates.

Finally, the TBMD simulations have also given an explanation of the surprising experimental result that at surface temperatures below 100 K O_2 molecules impinging on Pt(111) do not dissociate, even at kinetic energies up to 1.4 eV which are much greater than the dissociation barrier [83, 86, 87]. In fact, no single dissociation event was observed in the molecular dynamics simula-

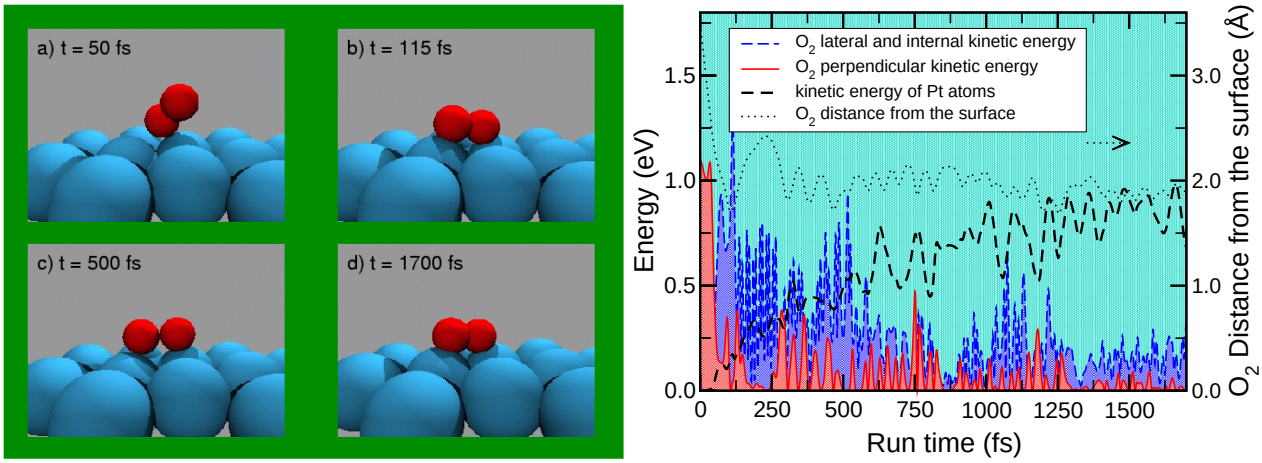

FIG. 13: TBMD trajectory of an O_2 molecule impinging on a Pt(111) surface with a kinetic energy of 1.1 eV. Left panel: four snapshots of the trajectory; right panel: distance from the surface and energy redistribution as a function of the run time. The lateral and internal kinetic energy and the perpendicular kinetic energy curves are indicated by the blue and red-shaded areas, respectively.

tions, irrespective of the initial energy. Again, there is a rather simple explanation in terms of the topology of the underlying PES. As far as the elbow potentials plotted in Fig. 10 are concerned, dissociation corresponds to an event in which the molecules enter the exit channel towards the lower right corner of the figures. However, there is a rather narrow curve connecting the entrance and exit channels through the molecular chemisorption states.

Now the molecules that enter the chemisorption well become accelerated towards the surface. This makes the molecules so fast that they "do not make it around the corner" into the dissociation channel. This is illustrated by the projection of a trajectory with $E_{\rm kin} = 0.6$ eV onto the Zd plane in Fig. 10a. This kinetic energy is much larger than the dissociation barrier. Still the molecule does not dissociate. Due to the acceleration by the attractive potential it hits the repulsive wall of the potential almost straight ahead and is reflected back.

This means that direct dissociation is sterically hindered at the Pt(111) surface so that it becomes a two-step process. First the molecule is trapped molecularly in the chemisorption well where it equilibrates. At sufficiently high surface temperatures dissociation will then be induced by thermal fluctuations which make the O_2 molecules enter the dissociation channel.

The TBMD results demonstrate that the molecular sticking probability of O_2/Pt(111) for the whole energy range can be understood in terms of trapping into the chemisorption states. However, these results can only be obtained and understood if the multidimensionality of the adsorption process is appropriately taken into account.

VII. ELECTRONICALLY NONADIABATIC EFFECTS IN THE ADSORPTION DYNAMICS

In all dynamical simulations presented so far it has been assumed that the electrons stay in their ground state throughout the whole process, i.e., the simulations have been based on the Born-Oppenheimer approximation. Still, at metal surfaces with their continuous spectrum of electronic states at the Fermi energy electron-hole (e-h) pair excitations with arbitrarily small energies are possible. However, the incorporation of electronically adiabatic effects in the dynamical simulation of the interaction dynamics of molecules with surface is rather difficult [2, 109]. Hence the role of electron-hole pairs in the adsorption dynamics as an additional dissipation channel is still unclear [4].

Recent experiments determining the so-called chemicurrent [111] have provided some information on the importance of electron-hole pair excitation in adsorption processes. Using thin films deposited on n-type Si(111) as a Schottky diode device, the nonadiabatically generated electron-hole pairs upon both atomic and molecular chemisorption create the chemicurrent which can be measured [111, 112]. It has been estimated that for example in the NO adsorption on Ag one quarter of the adsorption energy was dissipated to electron-hole pairs. Adsorption-induced electron hole-pair creation has also been found for other metal substrates, such as Au, Pt, Pd, Cu, Ni and Fe, and even for semiconductors such as GaAs and Ge [112, 113].

Since DFT calculations are in principle only applicable for the electronic ground state, they cannot be used in order to describe electronic excitations. Still it is possible to treat electronic exciations from first principles by either using quantum chemistry methods [114] or time-dependent density-functional theory (TDDFT)

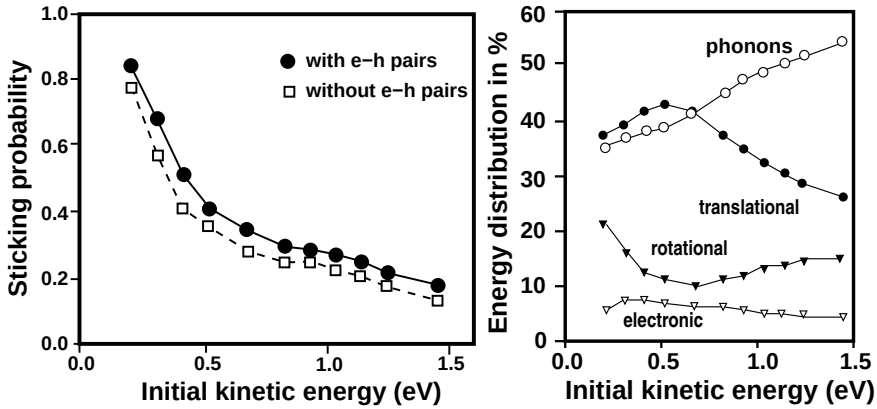

FIG. 14: Role of e–h pairs in the scattering and sticking of CO/Cu(111) at a surface temperature of $T_s = 100\,\mathrm{K}$; (**a**) sticking probability for CO/Cu(111) under normal incidence calculated without and with electronic friction, (**b**) Energy distribution of CO molecules scattered under normal incidence from Cu(111) in percent of the initial kinetic energy (after [110]).

[115, 116]. First attempts have been done in order to calculate the chemicurrent created by an atiom incident on a metal surface based on time-dependent density functional theory [117, 118]. In this approach, three independent steps are preformed. First, a conventional Kohn-Sham DFT calculations is performed in order to evaluate the ground state potential energy surface. Then, the resulting Kohn-Sham states are used in the framework of time-dependent DFT in order to obtain a position dependent friction coefficient. Finally, this friction coefficient is used in a forced oscillator model in which the probability density of electron-hole pair excitations caused by the classical motion of the incident atom is estimated.

This formalism has been employed [118] to address the chemicurrent measured in experiments of the adsorption of hydrogen atoms on copper surfaces [119]. Satisfactory agreement with the experiment has been obtained. However, only one single trajectory of a hydrogen atom impinging on the top site has entered the forced oscillator description so that the effect of corrugation has been entirely neglected.

Electron-hole pairs have already been treated on the Hartree-Fock level in otherwise classical high-dimensional molecular dynamics simulation using the *molecular dynamics with electronic friction* method [120]. In this approach, the energy transfer between nuclear degrees of freedom and the electron bath of the surface is also modelled with a position-dependent friction term, but additionally temperature-dependent fluctuating forces are included.

The friction term has been evaluated for CO/Cu(100) by Hartree-Fock cluster calculations using single excitations. A parametrized form of the Hartree-Fock results has been used for the molecular dynamics simulations. The interaction potential of CO/Cu(100) in the nuclear degrees of freedom, however, was derived empirically.

The sticking probability of CO/Cu(100) was determined by averaging over molecular dynamics trajectories with 108 surface atoms in the periodic surface unit cell and stochastic boundary conditions representing interactions with the bulk. The results with and without the consideration of e-h excitations are shown in Fig. 14a. Note that the sticking probability shows the typical monotonously decreasing behavior as a function of the kinetic energy. The incorporation of e-h pairs leads to an additional channel for energy transfer to the surface which results in a higher sticking probability. However, the effect is rather small. This means that e-h pair excitation plays only a minor role as a dissipation channel in the sticking and scattering of CO/Cu(100).

In order to quantify the energy transfer to the e-h pairs, the energy distribution for directly scattered molecules was determined (Fig. 14b). Less than 10% of the incident kinetic energy is transfered to e-h pairs in a direct scattering process which is less than observed for NO/Ag [112]. The main energy loss channel for CO/Cu(100) is the excitation of surface phonons. These findings can be rationalized by considering different time scales of electronic and nuclear motion which already entered the derivation of the Born-Oppenheimer approximation. Even if it takes infinitesimal energies to excite e-h pairs as in the case of metal surfaces, still their excitation probability is small compared to the excitation of surface phonons.

Nevertheless, it is not appropriate to naively generalize the results for the CO/Cu(100) system to other systems. Copper has almost no d-band density of states at the Fermi level; in addition, CO has a closed shell electronic configuration. For other substrate materials and molecules the coupling between surface e-h pairs and impinging molecules might be much stronger. For example, the observed stronger nonadiabatic dissipation effects in the system NO/Ag [112] might be caused by the unpaired electron in NO. There is certainly plenty of room for further investigations.

So far we have only focused in this section on electronic excitations in the substrate. However, there is a very important class of reactions at surfaces which involve localized electronic excitations at the adsorbate

or the adsorbate-surface bond [121, 122]. These reactions are often induced by electrons and photons. In particular, the *desorption induced by electronic transitions* (DIET) has been studied intensively, both experimentally as well as theoretically [121]. Most theoretical studies have in fact been based on empirical model potentials due to the problems associated with the first-principles determination of excited state potentials. Nevertheless, the dynamics of the laser-induced desorption of NO from NiO(100) [123] and of CO from Cr_2O_3 [124, 125] have already been addressed from first-principles. Using quantum chemical configuration interaction (CI) calculations, the ground state and one charge transfer PES of NO/NiO(100) has been determined for a restricted two-dimensional geometry. This PES has then been used as an input for jumping wave packet calculations. In this method, the wave packet is propagated on the excited state potential for a number of different lifetimes before it is transferred back to the ground state potential in a Franck-Condon transition. The final results are obtained by averaging over the simulations for different lifetimes which are weighted exponentially with a mean residence time.

These low-dimensional wave packet calculations have provided a qualitative explanation for the bimodality found experimentally in the velocity distribution of desorbing molecules [126]. The specific shape of the excited state PES leads to a bifurcation of the wave function in the excited state. The two parts of the wave function desorb with different mean velocities thus reproducing the bimodality.

The three-dimensional study of the photodesorption of CO from Cr_2O_3 confirmed the importance of including the angular coordinates in the simulations [124, 125]. The measured rotational alignment of the desorbing CO molecules could be reproduced qualitatively but quantitative discrepancies still remained. One of the challenging tasks for the future is to increase the dimensionality of the simulations in order to model the photo-induced desorption more realistically.

VIII. CONCLUSIONS AND OUTLOOK

In this review dynamical simulations of reactions at surfaces have been addressed which have utilized potential energy surfaces derived from first-principles electronic structure calculations. I have tried to show that such simulations have significantly deepened our understanding of the crucial microscopic reaction mechanisms occuring at surfaces. Not only a better quantitative agreement with the experiment has been achieved, but also novel qualitative mechanisms in the reaction dynamics at surfaces have been identified. The accuracy of many first-principles potential energy surfaces makes reliable predictions possible. Thus theory and experiment can cope with each other on an equal footing in the field of gas-surface dynamics. Furthermore, dynamical simulations have the great advantage that they allow a detailed microscopic analysis of the reaction mechanisms which is hard to achieve in experiments.

Still most dynamical simulations of reactions at surfaces are limited to rather simple systems, such as the adsorption of diatomic molecules on low-index single crystal surfaces. With the development of more efficient algorithms and the improvement of computer power, more and more complex systems will be able to be addressed. One recent example is the *ab initio* molecular dynamics simulation of the soft-landing of Pd_n clusters on oxide surfaces [127] where up to $n = 13$ Pd atoms have been taken into account in the calculations.

Most probably we will gain further exciting insights into the reaction dynamics at surfaces by first-principles simulations. Of course, it is hard to envisage which new qualitative concepts will emerge from these simulations; if one could predict this, the concepts would already be known. However, it is fair to say that there are still some open problems in the theoretical description of gas-surface dynamics. First of all, for some systems the *ab initio* potential energy surfaces are apparently seriously in error [128, 129]. In particular, the treatment of oxygen using current DFT exchange-corelation functionals is problematic [24]. Furthermore, an important class of reactions at surfaces involve electronic transitions. The theoretical description of electronically nonadiabatic reactions at surfaces from first principles is still in its infancy. It is not only the determination of excited state potentials which is difficult, but also the incorporation of electronic transitions in the reaction dynamics [109]. Last but not least, there are some systems such as reactions at the solid-liquid interface where hardly anything is known about the microscopic reaction dynamics.

It will be certainly worth-while to meet all these challenges. Dynamical simulations of molecule-surface interactions from first principles have been very successful in the past, and will continue to be so in the future.

[1] A. Groß, *Theoretical surface science – A microscopic perspective* (Springer, Berlin, 2002).
[2] A. Groß, Surf. Sci. Rep. **32**, 291 (1998).
[3] G.-J. Kroes, Prog. Surf. Sci. **60**, 1 (1999).
[4] G. R. Darling and S. Holloway, Rep. Prog. Phys. **58**, 1595 (1995).
[5] A. Groß, S. Wilke, and M. Scheffler, Phys. Rev. Lett. **75**, 2718 (1995).
[6] E. K. Grimmelmann, J. C. Tully, and M. J. Cardillo, J. Chem. Phys. **72**, 1039 (1980).
[7] E. W. Kuipers, M. G. Tenner, M. E. M. Spruit, and A. W. Kleyn, Surf. Sci. **205**, 241 (1988).
[8] A. Groß and M. Scheffler, J. Vac. Sci. Technol. A **15**, 1624 (1997).

[9] C. Crespos, H. F. Busnengo, W. Dong, and A. Salin, J. Chem. Phys. **114**, 10954 (2001).
[10] G.-J. Kroes, E. J. Baerends, and R. C. Mowrey, Phys. Rev. Lett. **78**, 3583 (1997).
[11] A. Groß, C.-M. Wei, and M. Scheffler, Surf. Sci. **416**, L1095 (1998).
[12] A. Eichler, J. Hafner, A. Groß, and M. Scheffler, Phys. Rev. B **59**, 13297 (1999).
[13] Y. Miura, H. Kasai, and W. Diño, J. Phys.: Condens. Matter **14**, L479 (2002).
[14] W. Brenig and M. F. Hilf, J. Phys. Condens. Mat. **13**, R61 (2001).
[15] A. Groß and M. Scheffler, Phys. Rev. B **57**, 2493 (1998).
[16] H. F. Busnengo, E. Pijper, M. F. Somers, G. J. Kroes, A. Salin, R. A. Olsen, D. Lemoine, and W. Dong, Chem. Phys. Lett. **356**, 515 (2002).
[17] G. R. Darling, Z. S. Wang, and S. Holloway, Phys. Chem. Chem. Phys. **2**, 911 (2000).
[18] S. Wilke and M. Scheffler, Phys. Rev. B **53**, 4926 (1996).
[19] S. Sakong and A. Groß, surf. Sci., accepted for publication.
[20] P. Hohenberg and W. Kohn, Phys. Rev. **136**, B864 (1964).
[21] W. Kohn and L. Sham, Phys. Rev. **140**, A1133 (1965).
[22] B. Hammer, M. Scheffler, K. Jacobsen, and J. Nørskov, Phys. Rev. Lett. **73**, 1400 (1994).
[23] J. P. Perdew, J. A. Chevary, S. H. Vosko, K. A. Jackson, M. R. Pederson, D. J. Singh, and C. Fiolhais, Phys. Rev. B **46**, 6671 (1992).
[24] B. Hammer, L. B. Hansen, and J. K. Nørskov, Phys. Rev. B **59**, 7413 (1999).
[25] K. D. Rendulic and A. Winkler, Surf. Sci. **299/300**, 261 (1994).
[26] W. Diño, H. Kasai, and A. Okiji, Prog. Surf. Sci. **63**, 63 (2000).
[27] H. A. Michelsen and D. J. Auerbach, J. Chem. Phys. **94**, 7502 (1991).
[28] C. T. Rettner, D. J. Auerbach, and H. A. Michelsen, Phys. Rev. Lett. **68**, 1164 (1992).
[29] D. Wetzig, R. Dopheide, M. Rutkowski, R. David, and H. Zacharias, Phys. Rev. Lett. **76**, 463 (1996).
[30] G. R. Darling and S. Holloway, J. Chem. Phys. **101**, 3268 (1994).
[31] A. Groß, B. Hammer, M. Scheffler, and W. Brenig, Phys. Rev. Lett. **73**, 3121 (1994).
[32] D. A. McCormack, G.-J. Kroes, R. A. Olsen, J. A. Groeneveld, J. N. P. van Stralen, E. J. Baerends, and R. C. Mowrey, Chem. Phys. Lett. **328**, 317 (2000).
[33] G. Anger, A. Winkler, and K. D. Rendulic, Surf. Sci. **220**, 1 (1989).
[34] C. T. Rettner, H. A. Michelsen, and D. J. Auerbach, J. Chem. Phys. **102**, 4625 (1995).
[35] A. De Vita, I. Štich, M. J. Gillan, M. C. Payne, and L. J. Clarke, Phys. Rev. Lett. **71**, 1276 (1993).
[36] A. J. R. da Silva, M. R. Radeke, and E. A. Carter, Surf. Sci. **381**, L628 (1997).
[37] A. Groß, M. Bockstedte, and M. Scheffler, Phys. Rev. Lett. **79**, 701 (1997).
[38] G. Wiesenekker, G.-J. Kroes, and E. J. Baerends, J. Chem. Phys. **104**, 7344 (1996).
[39] H. F. Busnengo, A. Salin, and W. Dong, J. Chem. Phys. **112**, 7641 (2000).
[40] G. Kresse, Phys. Rev. B **62**, 8295 (2000).
[41] A. Groß, M. Scheffler, M. J. Mehl, and D. A. Papaconstantopoulos, Phys. Rev. Lett. **82**, 1209 (1999).
[42] M. J. Mehl and D. A. Papaconstantopoulos, Phys. Rev. B **54**, 4519 (1996).
[43] C. M. Goringe, D. R. Bowler, and E. Hernández, Rep. Prog. Phys. **60**, 1447 (1997).
[44] K. D. Rendulic, G. Anger, and A. Winkler, Surf. Sci. **208**, 404 (1989).
[45] D. A. King, CRC Crit. Rev. Solid State Mater. Sci. **7**, 167 (1978).
[46] H. F. Busnengo, W. Dong, and A. Salin, Chem. Phys. Lett. **320**, 328 (2000).
[47] A. Groß, S. Wilke, and M. Scheffler, Surf. Sci. **357/358**, 614 (1996).
[48] M. Beutl, M. Riedler, and K. D. Rendulic, Chem. Phys. Lett. **247**, 249 (1995).
[49] M. Gostein and G. O. Sitz, J. Chem. Phys. **106**, 7378 (1997).
[50] D. Wetzig, M. Rutkowski, H. Zacharias, and A. Groß, Phys. Rev. B **63**, 205412 (2001).
[51] H. J. Kreuzer and Z. W. Gortel, *Physisorption Kinetics*, vol. 1 of *Springer Series in Surface Sciences* (Springer, Berlin, 1986).
[52] W. Brenig, *Nonequilibrium Thermodynamics* (Springer, Berlin, 1990).
[53] J. C. Polanyi and W. H. Wong, J. Chem. Phys. **51**, 1439 (1969).
[54] A. Groß and M. Scheffler, Chem. Phys. Lett. **256**, 417 (1996).
[55] L. Schröter, H. Zacharias, and R. David, Phys. Rev. Lett. **62**, 571 (1989).
[56] M. Karikorpi, S. Holloway, N. Henriksen, and J. K. Nørskov, Surf. Sci. **179**, L41 (1987).
[57] A. Groß, Appl. Phys. A **67**, 627 (1998).
[58] M. F. Somers, D. A. McCormack, G.-J. Kroes, R. A. Olsen, E. J. Baerends, and R. C. Mowrey, J. Chem. Phys. **117**, 6673 (2002).
[59] E. Watts, G. O. Sitz, D. A. McCormack, G.-J. Kroes, R. A. Olsen, J. A. Groeneveld, J. N. P. van Stralen, E. J. Baerends, and R. C. Mowrey, J. Chem. Phys. **114**, 495 (2001).
[60] Ž. Šljivančanin and B. Hammer, Phys. Rev. B **65**, 085414 (2002).
[61] K. W. Kolasinski, Int. J. Mod. Phys. B **9**, 2753 (1995).
[62] K. W. Kolasinski, W. Nessler, A. de Meijere, and E. Hasselbrink, Phys. Rev. Lett. **72**, 1356 (1994).
[63] P. Bratu, W. Brenig, A. Groß, M. Hartmann, U. Höfer, P. Kratzer, and R. Russ, Phys. Rev. B. **54**, 5978 (1996).
[64] F. M. Zimmermann and X. Pan, Phys. Rev. Lett. **85**, 618 (2000).
[65] P. Bratu and U. Höfer, Phys. Rev. Lett. **74**, 1625 (1995).
[66] M. Dürr, A. Biedermann, Z. Hu, U. Höfer, and T. F. Heinz, Science **296**, 1838 (2002).
[67] K. W. Kolasinski, W. Nessler, K.-H. Bornscheuer, and E. Hasselbrink, J. Chem. Phys. **101**, 7082 (1994).
[68] W. Brenig, A. Groß, and R. Russ, Z. Phys. B **96**, 231 (1994).
[69] P. Nachtigall, K. D. Jordan, A. Smith, and H. Jónsson, J. Chem. Phys. **104**, 148 (1996).
[70] E. Penev, P. Kratzer, and M. Scheffler, J. Chem. Phys. **110**, 3986 (1999).
[71] P. Kratzer, E. Pehlke, M. Scheffler, M. B. Raschke, and U. Höfer, Phys. Rev. Lett. **81**, 5596 (1998).

[72] E. Pehlke, Phys. Rev. B **62**, 12932 (2000).
[73] C. Filippi, S. B. Healy, P. Kratzer, E. Pehlke, and M. Scheffler, Phys. Rev. Lett. **89**, 166102 (2002).
[74] P. Bratu, K. L. Kompa, and U. Höfer, Chem. Phys. Lett. **251**, 1 (1996).
[75] A. Vittadini and A. Selloni, Chem. Phys. Lett. **235**, 334 (1995).
[76] P. Kratzer, B. Hammer, and J. K. Norskøv, Chem. Phys. Lett. **229**, 645 (1994).
[77] E. Pehlke and M. Scheffler, Phys. Rev. Lett. **74**, 952 (1995).
[78] E. Pehlke and P. Kratzer, Phys. Rev. B **59**, 2790 (1999).
[79] A. Biedermann, E. Knoesel, Z. Hu, and T. F. Heinz, Phys. Rev. Lett. **83**, 1810 (1999).
[80] T. Sagara, T. Kuga, K. Tanaka, T. Shibataka, T. Fujimoto, and A. Namiki, Phys. Rev. Lett. **89**, 086101 (2002).
[81] A. C. Luntz, M. D. Williams, and D. S. Bethune, J. Chem. Phys. **89**, 4381 (1988).
[82] W. Wurth, J. Stöhr, P. Feulner, X. Pan, K. R. Bauchspiess, Y. Baba, E. Hudel, G. Rocker, and D. Menzel, Phys. Rev. Lett. **65**, 2426 (1990).
[83] C. T. Rettner and C. B. Mullins, J. Chem. Phys. **94**, 1626 (1991).
[84] J. Wintterlin, R. Schuster, and G. Ertl, Phys. Rev. Lett. **77**, 123 (1996).
[85] B. C. Stipe, M. A. Rezaei, W. Ho, S. Gao, M. Persson, and B. I. Lundqvist, Phys. Rev. Lett. **78**, 4410 (1997).
[86] P. D. Nolan, B. R. Lutz, P. L. Tanaka, J. E. Davis, and C. B. Mullins, Phys. Rev. Lett. **81**, 3179 (1998).
[87] P. D. Nolan, B. R. Lutz, P. L. Tanaka, J. E. Davis, and C. B. Mullins, J. Chem. Phys. **111**, 3696 (1999).
[88] A. C. Luntz, J. Grimblot, and D. E. Fowler, Phys. Rev. B **39**, 12903 (1989).
[89] H. Steininger, S. Lehwald, and H. Ibach, Surf. Sci. **123**, 1 (1982).
[90] C. Puglia, A. Nilsson, B. Hernnäs, O. Karis, P. Bennich, and N. Mårtensson, Surf. Sci. **342**, 119 (1995).
[91] A. Eichler and J. Hafner, Phys. Rev. Lett. **79**, 4481 (1997).
[92] A. Eichler, F. Mittendorfer, and J. Hafner, Phys. Rev. B **62**, 4744 (2000).
[93] J. C. Slater and G. F. Koster, Phys. Rev. **94**, 1498 (1954).
[94] D. J. Chadi, Phys. Rev. B **19**, 2074 (1979).
[95] A. P. Sutton, M. W. Finnis, D. G. Pettifor, and Y. Ohta, J. Phys. C: Solid State Phys. **21**, 35 (1988).
[96] M. Desjonquères and D. Spanjaard, *Concepts in Surface Physics* (Springer, Berlin, 1996), 2nd ed.
[97] M. Elstner, D. Porezag, G. Jungnickel, J. Elsner, M. Haugk, T. Frauenheim, S. Suhai, and G. Seifert, Phys. Rev. B **58**, 7260 (1998).
[98] L. Goodwin, A. J. Skinner, and D. G. Pettifor, Europhys. Lett. **9**, 701 (1989).
[99] A. Groß, A. Eichler, J. Hafner, M. J. Mehl, and D. A. Papaconstantopoulos, submitted.
[100] WWW address: http://cst-www.nrl.navy.mil/bind.
[101] F. Kirchhoff, M. J. Mehl, N. I. Papanicolaou, D. A. Papaconstantopoulos, and F. S. Khan, Phys. Rev. B **63**, 195101 (2001).
[102] The TBMD simulations have mainly been performed at the Cray T3E of the John-von-Neumann center for scientific computing.
[103] S. A. Adelman and J. D. Doll, J. Chem. Phys. **64**, 2375 (1976).
[104] S. Nosé, J. Chem. Phys. **81**, 511 (1984).
[105] W. G. Hoover, *Molecular Dynamics*, vol. 258 of *Lecture Notes in Physics* (Springer, Berlin, 1986).
[106] P. Gambardella, Ž. Šljivančanin, B. Hammer, M. Blanc, K. Kuhnke, and K. Kern, Phys. Rev. Lett. **87**, 056103 (2001).
[107] J. L. Gland, B. A. Sexton, and G. B. Fisher, Surf. Sci. **95**, 587 (1980).
[108] M. Beutl, K. D. Rendulic, and G. R. Castro, Surf. Sci. **385**, 97 (1997).
[109] C. Bach and A. Groß, J. Chem. Phys. **114**, 6396 (2001).
[110] J. T. Kindt, J. C. Tully, M. Head-Gordon, and M. A. Gomez, J. Chem. Phys. **109**, 3629 (1998).
[111] H. Nienhaus, Surf. Sci. Rep. **45**, 1 (2002).
[112] B. Gergen, H. Nienhaus, W. H. Weinberg, and E. W. McFarland, Science **294**, 2521 (2001).
[113] B. Gergen, S. J. Weyers, H. Nienhaus, W. H. Weinberg, and E. W. McFarland, Surf. Sci. **488**, 123 (2001).
[114] M. Head-Gordon, J. Phys. Chem. **100**, 13213 (1996).
[115] E. Runge and E. Gross, Phys. Rev. Lett. **52**, 997 (1984).
[116] E. K. U. Gross, J. F. Dobson, and M. Petersilka, in *Density functional theory*, edited by R. F. Nalewajski (Springer, Berlin, 1996), vol. 181 of *Topics in Current Chemistry*, p. 81.
[117] J. R. Trail, M. C. Graham, and D. M. Bird, Comp. Phys. Comm. **137**, 163 (2001).
[118] J. R. Trail, M. C. Graham, D. M. Bird, M. Persson, and S. Holloway, Phys. Rev. Lett. **88**, 166802 (2002).
[119] H. Nienhaus, H. S. Bergh, B. Gergen, A. Majumdar, W. H. Weinberg, and E. W. McFarland, Phys. Rev. Lett. **82**, 466 (1999).
[120] M. Head-Gordon and J. C. Tully, J. Chem. Phys. **103**, 10137 (1995).
[121] H. Guo, P. Saalfrank, and T. Seideman, Prog. Surf. Sci. **62**, 239 (1999).
[122] J. C. Tully, Annu. Rev. Phys. Chem. **51**, 153 (2000).
[123] T. Klüner, H.-J. Freund, V. Staemmler, and R. Kosloff, Phys. Rev. Lett. **80**, 5208 (1998).
[124] S. Thiel, M. Pykavy, T. Klüner, H.-J. Freund, and R. Kosloff, Phys. Rev. Lett. **87**, 077601 (2001).
[125] S. Thiel, M. Pykavy, T. Klüner, H.-J. Freund, R. Kosloff, and V. Staemmler, J. Chem. Phys. **116**, 762 (2002).
[126] T. Mull, B. Baumeister, M. Menges, H.-J. Freund, D. Weide, C. Fischer, and P. Andresen, J. Chem. Phys. **96**, 7108 (1992).
[127] M. Moseler, H. Häkkinen, and U. Landman, Phys. Rev. Lett. **89**, 176103 (2002).
[128] P. J. Feibelman, B. Hammer, J. K. Nørskov, F. Wagner, M. Scheffler, R. Stumpf, R. Watwe, and J. Dumesic, J. Phys. Chem. B **105**, 4018 (2001).
[129] Y. Y. Yourdshahyan, B. Razaznejad, and B. I. Lundqvist, Phys. Rev. B **65**, 075415 (2002).